

## Pressure and temperature dependence of the dielectric properties of $\text{CsH}_2\text{PO}_4$ and $\text{CsD}_2\text{PO}_4$

Naohiko Yasuda, Sanji Fujimoto, Motohide Okamoto, and Hiroyasu Shimizu  
*Department of Electrical Engineering, Gifu University, Gifu, Japan*

Katsumi Yoshino and Yoshio Inuishi  
*Department of Electrical Engineering, Osaka University, Osaka, Japan*  
 (Received 12 March 1979)

The pressure (0–7 kbar) and temperature (–200–+10 °C) dependence of the dielectric properties (relative permittivity  $\epsilon_r$  and spontaneous polarization  $P_s$ ) of  $\text{CsH}_2\text{PO}_4$  and  $\text{CsD}_2\text{PO}_4$  were investigated. By the observation of the  $P$ - $E$  double hysteresis loops it is confirmed that the pressure-induced phase (at pressures above the critical pressure  $p_c$ ) is antiferroelectric for both compounds. The pressure-temperature phase diagrams of both compounds were dielectrically determined. The pressure effects on the dielectric properties were found to be striking in comparison with those of the other  $\text{KH}_2\text{PO}_4$ -type crystals: (i) the  $P_s$  and the Curie constant decrease strongly with pressure at pressures below  $p_c$ ; and (ii) the critical electric field which induces the forced transition has a very small value and its pressure dependence is very large at pressures above  $p_c$ . Such facts reflect the one-dimensional nature characterized by the chainlike ordering of the hydrogen bonds along the  $b$  axis. The dielectric properties associated with the paraelectric-ferroelectric and -antiferroelectric transitions are explained by introducing into an Ising spin model (containing the proton tunneling) a spin-spin interaction term within the chain and an interaction term between spins among the chains along the  $b$  axis.

### I. INTRODUCTION

In the paraelectric phase cesium dihydrogen phosphate  $\text{CsH}_2\text{PO}_4$  [abbreviated CDP] belongs to the space group  $P2_1/m$  in the monoclinic system and undergoes a phase transition from the paraelectric to the ferroelectric phase at –120 °C at atmospheric pressure with cooling.<sup>1–4</sup> There is a large isotope effect on the transition temperature ( $T_c$ ) by substitution of deuterium for hydrogen, and the  $T_c^d$  is  $\sim -6$  (Ref. 3) to –8.5 °C (Refs. 5 and 6) for the deuterated analog  $\text{CsD}_2\text{PO}_4$  [abbreviated  $d$ -CDP] which is isostructural with CDP.<sup>5</sup> The transition temperatures for both compounds have recently been reported to decrease with increasing pressure ( $p$ ) with a slope  $dT_c/dp = -5.6$  (Ref. 6) or –8.5 °C/kbar (Ref. 7) for CDP and  $dT_c^d/dp = -8.5$  °C/kbar for  $d$ -CDP.<sup>6</sup> Such behavior for CDP suggests that the phase transition in CDP as well as in  $\text{KH}_2\text{PO}_4$  [abbreviated KDP] is microscopically explained by the tunneling model for the proton.<sup>6,8</sup> Despite these similarities, CDP has been found by neutron scattering studies<sup>5,9</sup> to have one-dimensional (1-D) nature characterized by the chainlike ordering of the hydrogen bond parallel to the ferroelectric  $b$  axis, and found by dielectric study under hydrostatic pressure<sup>7</sup> to have a new antiferroelectric phase induced by pressure as small as about 3.3 kbar. The change from the paraelectric-ferroelectric to the paraelectric-antiferroelectric transition has been suggested to originate from the 1-D na-

ture in CDP.<sup>7</sup> Such a characteristic of CDP sets it apart from the KDP family.

Many studies under pressure<sup>8,10</sup> on KDP-type crystals such as KDP,<sup>11</sup>  $\text{NH}_4\text{H}_2\text{PO}_4$  [abbreviated ADP]<sup>12</sup> and  $\text{RbH}_2\text{PO}_4$  [abbreviated RDP]<sup>13</sup> have been made, and the importance of pressure (or volume) as a variable in studying the properties of these crystals has been emphasized in them. Especially, Samara<sup>12</sup> demonstrated that the paraelectric-ferroelectric phase transition of KDP could be suppressed by the application of hydrostatic pressure. The vanishing of the ferroelectric state was qualitatively described by considering the effect of pressure on the important parameters of the tunneling model, namely, on the proton-tunneling frequency and the dipolar proton-proton interaction energy, etc.<sup>12</sup> For CDP and  $d$ -CDP, pressure induced a new antiferroelectric phase<sup>7</sup> and a new phase,<sup>6</sup> respectively. In the present work, we performed a detailed study of the pressure and temperature dependence of the dielectric properties of CDP and  $d$ -CDP, and found the pressure-induced antiferroelectric phase not only in CDP but also in  $d$ -CDP. The purpose of this paper is (a) to present detailed experimental results of these crystals, (b) to clarify the difference of the pressure effects on the dielectric properties between these crystals and other KDP-type crystals, and (c) to explain the dielectric properties under pressure and the pressure-induced antiferroelectricity resulting from the 1-D nature in CDP and  $d$ -CDP by using the pseudospin Ising model.

## II. EXPERIMENTAL METHOD

The compound CDP was synthesized by the reaction  $\text{Cs}_2\text{CO}_3 + 2\text{H}_3\text{PO}_4 = 2\text{CsH}_2\text{PO}_4 + \text{H}_2\text{O} + \text{CO}_2$ . Single crystals were grown from an aqueous solution by the slow evaporation method at room temperature. The acidity of the solution was controlled at about  $\text{pH} = 3.3$  by the addition of phosphoric acid.<sup>4</sup> For deuterated analog *d*-CDP, a similar procedure was followed in a nitrogen gas. Deuterated phosphoric acid (deuteration rate 99%) was supplied by E. Merk Co. Ltd. The transition temperature of deuterated compound obtained in this manner was about  $-11^\circ\text{C}$  and this value is slightly lower than the values reported previously.<sup>3,5,6</sup> This variation may be due to some small difference in the degree of sample deuteration. A plate perpendicular to the *b* axis was cut out with a beryllium wire cutter from a single crystal and was mirror polished with No. 1500  $\text{Al}_2\text{O}_3$  powder and gold was evaporated on its surfaces to act as electrodes. Each specimen was covered with a silicone varnish to protect it from moisture. The electrical capacitance of the specimen was measured at 1 kHz with a field smaller than 1 V/cm using a LCR (inductance, capacitance, resistance) meter and the spontaneous polarization was examined with an ordinary Sawyer-Tower circuit. In this case, the 60-Hz ac electric field was applied to the specimen as pulses for only 1 sec. A Cu-Be high-pressure vessel with 1:1 mixture of normal- and isopentane as a pressure transmitting fluid was used in order to apply the hydrostatic pressure to the specimen. The pressure vessel was placed in a conventional low-temperature Dewar. The vessel was fairly massive which helped to minimize any temperature gradients. The pressure was measured with Manganin gauges to an accuracy of  $\pm 1.5\%$ . The temperature was varied by positioning the vessel in the vapor above the liquid nitrogen in the Dewar. The temperature of the specimen was measured with a potentiometer with a calibrated Cu-Constantan thermocouple set closely to one of the electrodes. All of the dielectric data were gathered for varying temperature at a rate of  $0.1^\circ\text{C}/\text{min}$  under various constant pressures. All of the observed data are reversible on lowering pressure with good reproducibility, and therefore the pressure applied to the specimen may be hydrostatic in spite of the increase in the viscosity of a pressure-transmitting fluid at low temperatures.

## III. EXPERIMENTAL RESULTS

### A. $\text{CsH}_2\text{PO}_4$ and $\text{CsD}_2\text{PO}_4$

#### 1. Permittivity

As for CDP, the value of the Curie constant was reported to be ten times as large as that of KDP,<sup>1,3</sup> and the ferroelectric phase transition was suggested to be of first order though close to being a second-

order one because of the small difference between the transition temperature ( $T_c$ ) and the characteristic temperature ( $T_{c0}$ ) where the reciprocal relative permittivity is zero.<sup>3</sup> However, the heat anomaly at  $T_c$  at atmospheric pressure could not be detected by the DTA (differential thermal analysis) method with the highly sensitive Ag-Ge thermocouple. On the other hand, as for *d*-CDP, the pressure-temperature phase diagram has dielectrically been determined by Gesi,<sup>6</sup> but the permittivity versus temperature under pressure has not been reported. The *p*-*T* phase diagram of *d*-CDP obtained by us is similar to that obtained by Gesi.<sup>6</sup> Figures 1 and 2 show the temperature dependence of the relative permittivity along the ferroelectric *b* axis ( $\epsilon_r$ ) of CDP and *d*-CDP, respectively, under various constant pressures. It is found in Figs. 1 and 2 that the value of  $\epsilon_r$  changes strikingly at the critical pressure  $p_c = 3.3$  kbar for CDP or  $p_c^d = 5.2$  kbar for *d*-CDP.

At pressures lower than  $p_c$  or  $p_c^d$ , the  $\epsilon_r$  in the paraelectric phase above  $T_c$  or  $T_c^d$  obeys the Curie-Weiss law. The values of  $T_c$  and  $T_c^d$  decrease linearly

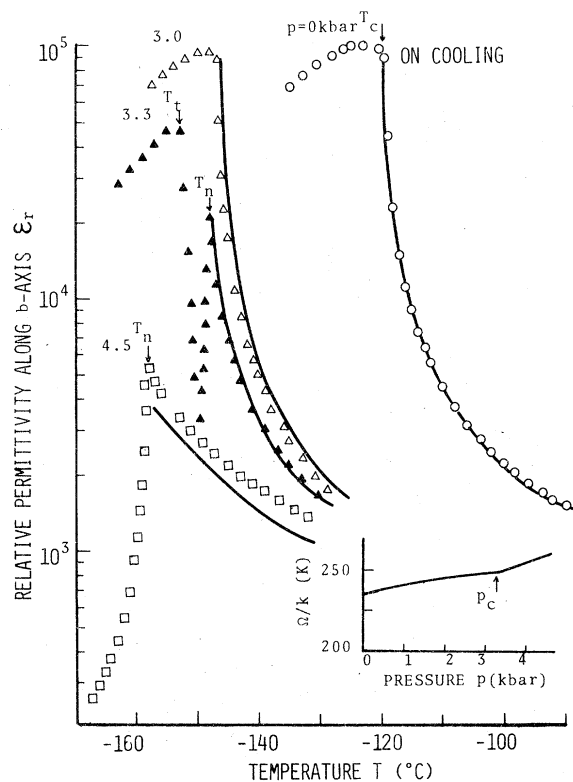


FIG. 1. Temperature dependence of the relative permittivity along the *b* axis ( $\epsilon_r$ ) of  $\text{CsH}_2\text{PO}_4$  measured at 1 kHz with a field smaller than 1 V/cm under constant pressures. The solid curves show the values of  $\epsilon_r$  calculated from Eqs. (2) and (11). The inset shows the pressure dependence of the tunneling integral ( $\Omega/k$ ) calculated from Eqs. (1) ( $p < p_c$ ) and (9) ( $p > p_c$ ), where  $p_c$  is the critical pressure.

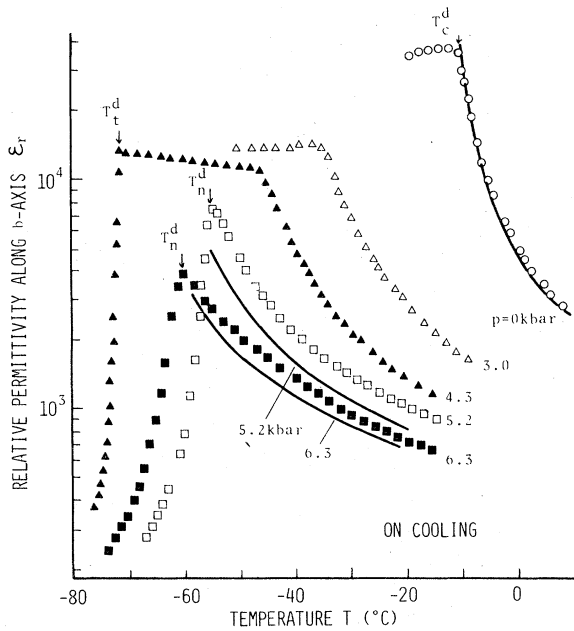


FIG. 2. Temperature dependence of the relative permittivity along the  $b$  axis ( $\epsilon_r$ ) of  $\text{CsD}_2\text{PO}_4$  measured at 1 kHz with a field smaller than 1 V/cm under constant pressures. The solid curves show the values of  $\epsilon_r$  calculated from Eqs. (2) and (11).

with increasing pressure and their pressure derivatives are listed in Table I. The values of Curie constants,  $C$  and  $C^d$ , decrease rapidly with increasing pressure as shown in Table I, and the values of their decreasing rate are very large in comparison with those in other KDP-type crystals such as RDP,<sup>13</sup> KDP,<sup>10</sup> and  $d$ -KDP<sup>10,14</sup> (see Table I). While the peak value of  $\epsilon_r$  ( $\epsilon_{r, \text{max}}$ ) for CDP decreases slightly with increasing pressure, the value of  $\epsilon_{r, \text{max}}$  for  $d$ -CDP decreases steeply (see Figs. 1 and 2). Levstik *et al.*<sup>3</sup> suggested that the transition at  $p = 1$  bar in  $d$ -CDP is of first order because of a difference of 11 °C between  $T_c^d$  and the characteristic temperature ( $T_{c0}^d$ ). Our present data indicate the small difference of 2.8 °C between  $T_c^d$  and  $T_{c0}^d$  at  $p = 1$  bar (see Fig. 2). The decrease of  $\epsilon_{r, \text{max}}$  for  $d$ -CDP comes from the increase in this difference ( $T_c^d - T_{c0}^d$ ) and the decrease in  $C^d$  with pressure.

At pressures near  $p_c$  or  $p_c^d$ , for CDP two peaks appear with cooling; one is at  $T_n$  and the other at  $T_t$  (see Fig. 1). As we compare the two peaks we find that (a) the peak value of  $\epsilon_r$  at  $T_n$  is lower than that at  $T_t$ ; (b) the value of  $\epsilon_r$  around  $T_n$  varies more steeply below  $T_n$  than above  $T_n$ ; (c) the value of  $\epsilon_r$  around  $T_t$  varies more steeply at  $T > T_t$  than at  $T < T_t$ ; (d) the behavior of  $\epsilon_r$  around  $T_t$  is similar to that around  $T_c$  at pressures below  $p_c$ ; and (e) the

TABLE I. Transition temperature  $T_c$ , its pressure derivative, and pressure derivatives of the Curie constant  $C$ , the spontaneous polarization  $P_s$ , and the loop height  $P_{\text{LH}}$  (see text) for paraelectric-ferroelectric and -antiferroelectric transitions for CDP and  $d$ -CDP. The earlier data on KDP,  $d$ -KDP, and RDP are also included.

	Paraelectric-ferroelectric transition				$T_n$ (K)	Paraelectric-antiferroelectric transition		
	$T_c$ (K)	$dT_c/dp$ (K/kbar)	$d \ln C/dp$ (%/kbar)	$d \ln P_s/dp$ (%/kbar)		$dT_n/dp$ (K/kbar)	$dC/dp$ (%/kbar)	$d \ln P_{\text{LH}}/dp$ (%/kbar)
CDP	153	-8.5 (-5.5)	-7	-6 <sup>a</sup>	125 (at $p_c$ )	-6.7 (-5.4)	$dC/dp > 0$ $C = 4.16 \text{ U}^b$ at 4 kbar $4.43 \text{ U}^b$ at 4.5 kbar	-1 <sup>a</sup>
$d$ -CDP	262	-8.5 (-3.2)	-4	-4 <sup>a</sup>	218 (at $p_c^d$ )	-2.5 (-1.2)	$dC^d/dp < 0$ $C^d = 4.24 \text{ U}^b$ at 5.2 kbar $3.81 \text{ U}^b$ at 6.3 kbar	-1 <sup>a</sup>
KDP <sup>c</sup>	122	-4.6 (-3.8)	-0.7	-1.55 <sup>d</sup>				
$d$ -KDP <sup>c</sup>	220	-2.5 (-1.1)	-1.5 <sup>e</sup>	-0.8				
RDP <sup>f</sup>	141	-6.2 (-4.4)	-0.9	-1.59				

<sup>a</sup>The value is estimated at  $T \ll T_{c \text{ or } n}$ .

<sup>b</sup> $\text{U} = 10^{-7} \text{ K F/m}$ .

<sup>c</sup>Reference 10.

<sup>d</sup>Reference 11.

<sup>e</sup>Reference 14.

<sup>f</sup>Reference 13.

slope  $dT_i/dp$  has a very large negative value. As for  $d$ -CDP, a steep decrease in  $\epsilon_r$  is observed at temperatures ( $T_i^d$ ) below  $T_c^d$  with cooling (see Fig. 2), and this fact demonstrates that a first-order phase transition occurs at  $T_i^d$ . With increasing pressure, this transition temperature ( $T_i^d$ ) increases with a slope  $dT_i^d/dp \cong 35^\circ\text{C/kbar}$  and the value of  $\epsilon_r$  at  $T_i^d$  decreases. Moreover the value of  $T_i^d$  coincides with  $T_c^d$  at  $p_c^d$  [triple point;  $p_c^d = 5.2 \pm 0.2$  kbar,  $T_c^d = -(55.2 \pm 0.3)^\circ\text{C}$ ].

At pressures above  $p_c$  or  $p_c^d$ , the peak of  $\epsilon_r$  at  $T_n$  or  $T_n^d$  appears with cooling. With increasing pressure, the values of  $T_n$  and  $T_n^d$  decrease linearly and their pressure derivatives are listed in Table I. The value of  $\epsilon_r$  at  $T$  above  $T_n$  or  $T_n^d$  follows the Curie-Weiss law. While the value of  $C$  for CDP increases with pressure, that for  $d$ -CDP decreases with pressure as shown in Table I. The peak value of  $\epsilon_r$  at  $T_n$  or  $T_n^d$  decreases with increasing pressure. This decrease in  $\epsilon_{r, \text{max}}$  results from mainly the increase in the difference between  $T_n$  or  $T_n^d$  and the characteristic temperature ( $T_{n0}$  or  $T_{n0}^d$ ) with pressure. The variation of  $1/\epsilon_r$  vs  $T$  near  $T_n$  or  $T_n^d$  appears discontinuous at  $T_n$  or  $T_n^d$ ; thus the transition at  $T_n$  or  $T_n^d$  may be of first order.

## 2. Spontaneous polarization

By the observation of the polarization ( $P$ )–electric field ( $E$ ) hysteresis loop, the phases at  $p < p_c$  and  $T < T_c$  for CDP and at  $p < p_c^d$  and  $T_i^d < T < T_c^d$  for  $d$ -CDP are confirmed to be ferroelectric. Figures 3 and 4 show the temperature dependence of the spontaneous polarization ( $P_s$ ) under various constant pressures for CDP and  $d$ -CDP, respectively, obtained from  $P$ - $E$  hysteresis loops. With cooling, the value of  $P_s$  increases rapidly near  $T_c$  or  $T_c^d$  and then gradually and finally slightly even at low temperatures to about  $-200^\circ\text{C}$ . The values of  $P_s$  decrease with increasing pressure and their decreasing rates are listed in Table I. These values are very large in comparison with

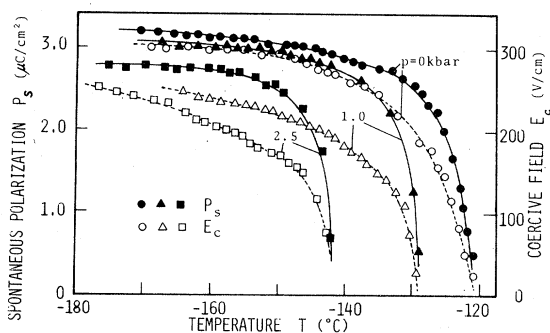


FIG. 3. Temperature dependence of the spontaneous polarization ( $P_s$ ) and the coercive field ( $E_c$ ) along the  $b$  axis of  $\text{CsH}_2\text{PO}_4$  under constant pressures.

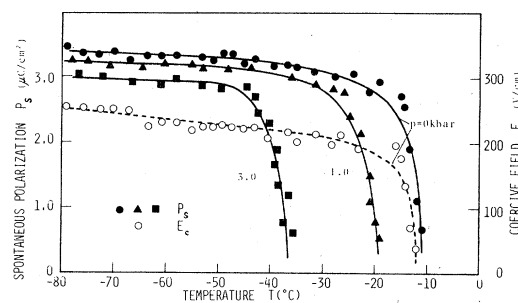


FIG. 4. Temperature dependence of the spontaneous polarization ( $P_s$ ) and the coercive field ( $E_c$ ) along the  $b$  axis of  $\text{CsD}_2\text{PO}_4$  under constant pressures.

those for  $\text{KDP}^{10,11}$  and  $\text{RDP}^{13}$  (see Table I). With cooling, the coercive field ( $E_c$ ) increases rapidly near  $T_c$  or  $T_c^d$  and then gradually as also seen in Figs. 3 and 4. The value of  $E_c$  has the tendency to decrease with pressure similarly to  $P_s$ . At pressures above  $p_c$  or  $p_c^d$ ,  $P$ - $E$  double hysteresis loops which are characteristic of antiferroelectrics were observed (see Fig. 5). With heating, the area and the height of the double hysteresis loop get smaller, and then on passing through the transition temperature the loop disappears and finally the  $P$ - $E$  relation becomes a straight line. It is noted that the critical electric field ( $E_{\text{cri}}$ ) estimated as the value of the field at the center of a loop has a very small value in comparison with those of the usual hydrogen-bonded antiferroelectrics,<sup>15</sup> for example,  $E_{\text{cri}} = 0.42$  kV/cm at  $p = 3.7$  kbar at  $T = -157^\circ\text{C}$  for CDP. Let the loop height of the double hysteresis loop be  $P_{\text{LH}}$  [see Fig. 6(a)]. The value of  $P_{\text{LH}}$  may correspond to twice the magnitude of the spontaneous polarization of a sublattice.<sup>16</sup> The temperature dependence of  $P_{\text{LH}}$  and  $E_{\text{cri}}$  under various constant pressures obtained from  $P$ - $E$  double hysteresis loops are shown in Figs. 6(a) and (b), respectively, for CDP and in Figs. 7(a) and (b) for  $d$ -CDP. With cooling, the value of  $P_{\text{LH}}$  increases rapidly near  $T_n$  or  $T_n^d$ , then gradually and finally shows a tendency to saturate. With increasing pressure, the value of  $P_{\text{LH}}$  decreases as shown in Table I. With cooling, the value of  $E_{\text{cri}}$  also increases steeply near  $T_n$  or  $T_n^d$  and then shows a tendency to saturate. It is noted that the pressure dependence of  $E_{\text{cri}}$  is strikingly large while that of  $P_{\text{LH}}$  is small. The  $P$ - $E$  relation of the antiferroelectric to the ferroelectric phase with cooling at a constant pressure is shown for CDP in Fig. 8. It is clearly seen in Fig. 8 that the  $P$ - $E$  hysteresis loop changes from a double hysteresis loop to a single loop. Thus the value of  $P_s$  at zero external electric field seems to change discontinuously from zero to a finite value at the transition temperature  $T_i$  or  $T_i^d$ . This fact suggests that the antiferroelectric-ferroelectric phase transition at  $T_i$  or  $T_i^d$  (Ref. 6) is of first order.

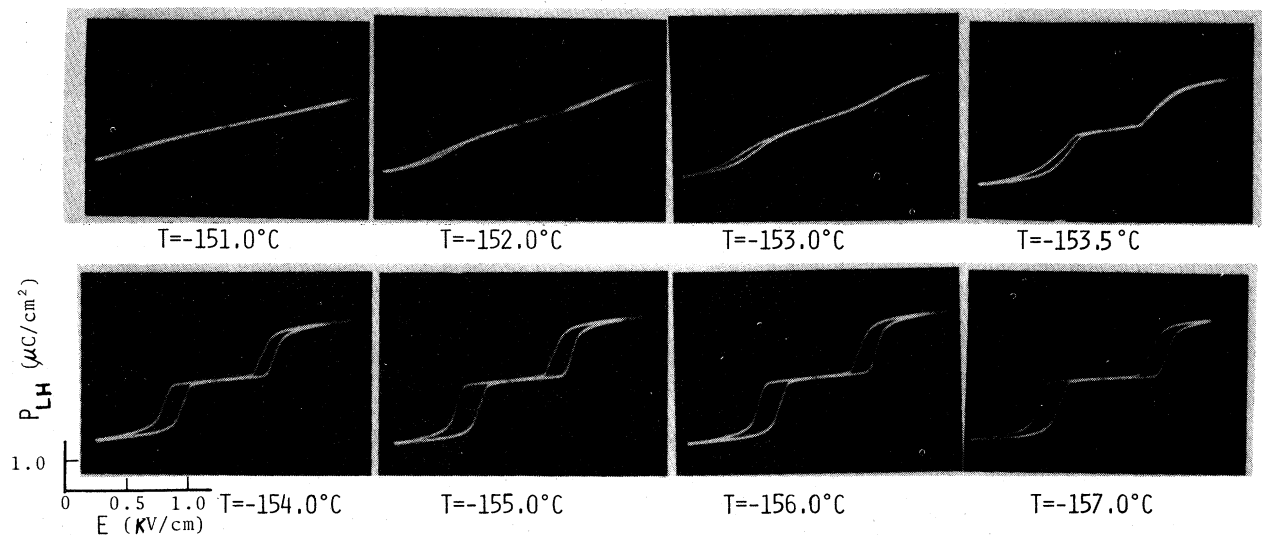


FIG. 5.  $P$ - $E$  double hysteresis loops at  $p = 3.7$  kbar with an ac amplitude of  $1.1$  kV/cm, along the  $b$  axis of  $\text{CsH}_2\text{PO}_4$  at various temperatures.

As mentioned above, the dielectric properties of  $d$ -CDP under pressures are qualitatively similar to those of CDP. However, the difference in the dielectric properties between CDP and  $d$ -CDP is summarized as follows: (i) the various transition temperatures of CDP are increased strikingly by deuteration,

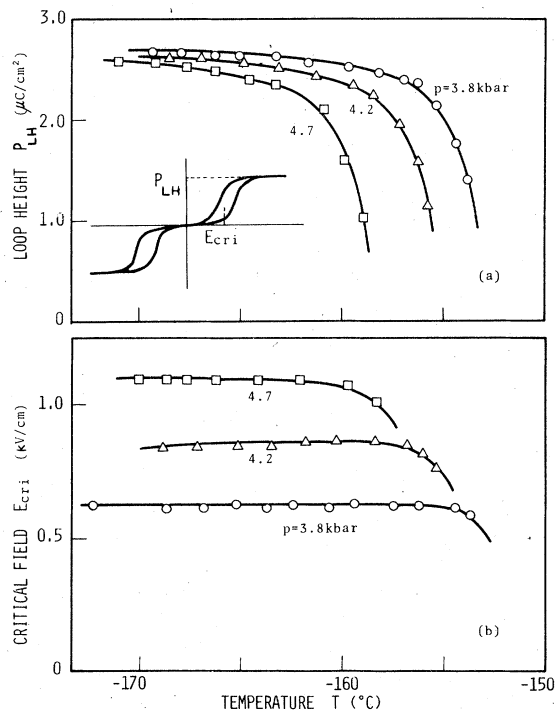


FIG. 6. Temperature dependence of (a) the loop height ( $P_{LH}$ ) and (b) the critical electric field ( $E_{cri}$ ) of the double hysteresis loop along the  $b$  axis of  $\text{CsH}_2\text{PO}_4$  under constant pressures.

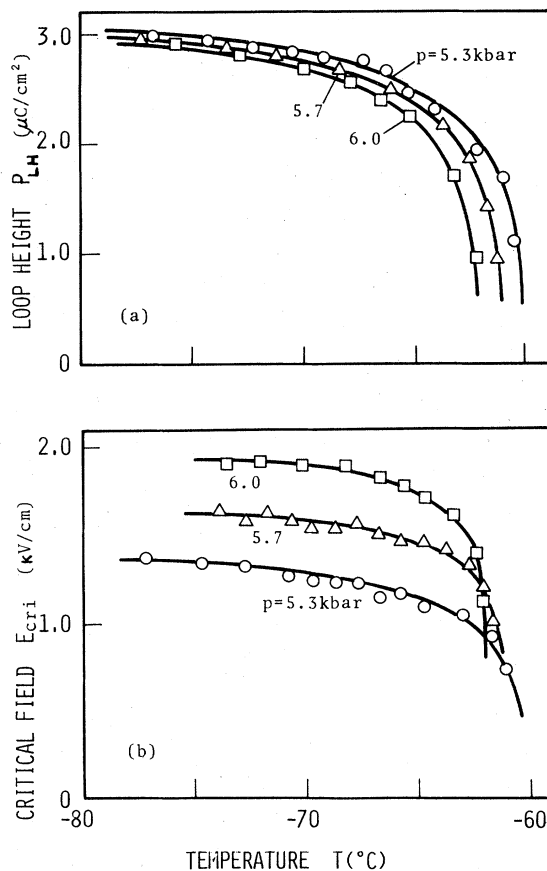


FIG. 7. Temperature dependence of (a) the loop height ( $P_{LH}$ ) and (b) the critical electric field ( $E_{cri}$ ) of the double hysteresis loop along the  $b$  axis of  $\text{CsD}_2\text{PO}_4$  under constant pressures.

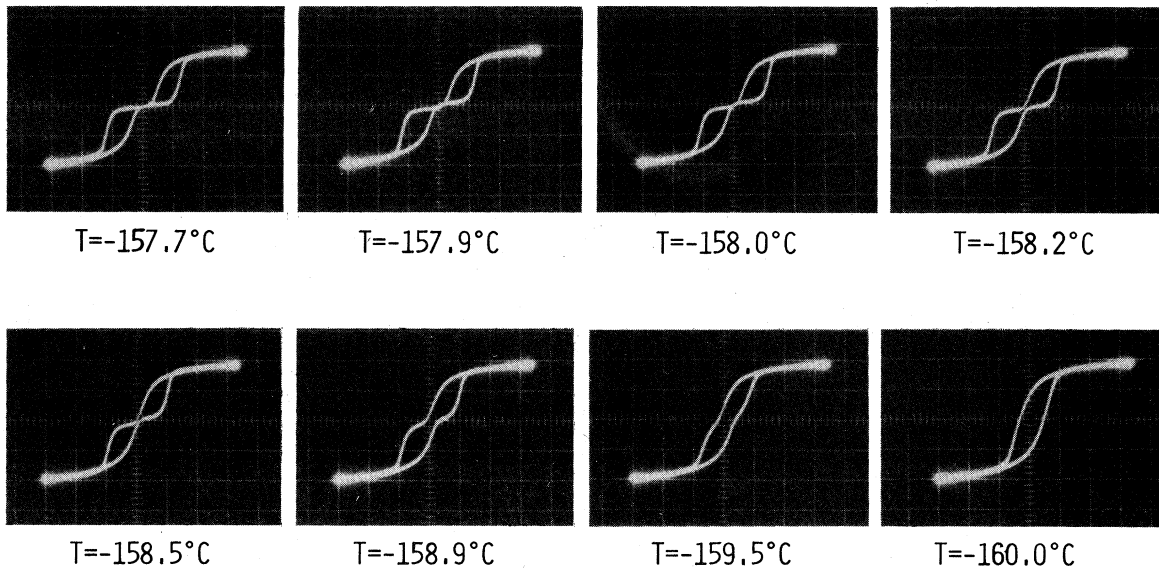


FIG. 8.  $P$ - $E$  relation of the antiferroelectric phase to the ferroelectric one along the  $b$  axis of  $\text{CsH}_2\text{PO}_4$  at the pressure just above  $p_c$  with cooling.

for example, the triple point is at  $p = 3.3 \pm 0.2$  kbar and  $T = -(148.5 \pm 0.3)^\circ\text{C}$  for CDP and is at  $p = 5.2 \pm 0.2$  kbar and  $T = -(55.2 \pm 0.3)^\circ\text{C}$  for  $d$ -CDP; (ii)  $dT_i/dp$  for the ferroelectric-antiferroelectric transition temperature ( $T_i$ ) is very large and negative for CDP, but is large and positive for  $d$ -CDP; (iii) the pressure effect on the  $\epsilon_r$  at the paraelectric-ferroelectric transition temperature ( $T_c$ ) is much larger in  $d$ -CDP than that in CDP; (iv) the pressure effect on the Curie constant in the antiferroelectric phase is positive ( $dC/dp > 0$ ) for CDP and negative ( $dC/dp < 0$ ) for  $d$ -CDP; and (v) near the triple point, the value of  $E_{\text{crit}}$  in the antiferroelectric phase is larger for  $d$ -CDP than for CDP.

#### B. Comparison with other $\text{KH}_2\text{PO}_4$ -type crystals

We will clarify the notable differences in the dielectric properties between CDP and other KDP-type crystals as follows: (i) While the qualitative change from the paraelectric-ferroelectric to the paraelectric-antiferroelectric transition in the CDP crystal is observed by a small pressure ( $p_c = 3.3$  kbar for CDP and  $p_c^d = 5.2$  kbar for  $d$ -CDP), such a qualitative change of a paraelectric-ferroelectric transition in the other KDP-type crystals by applying pressure has not been yet observed.<sup>8,10-13,17</sup> (ii) In the pressure-induced antiferroelectric phase in CDP crystals, the critical electric field by which the arrangement of polarizations can be changed from antiparallel to parallel is very small in comparison with those in the antipolar  $\text{ADP}^{15}$  and the hydrogen-bonded antiferroelectric  $\text{Cu}(\text{HCOO})_2 \cdot 4\text{H}_2\text{O}$ .<sup>15</sup> [Facts (i) and (ii) indicate the

weak three-dimensional correlation of polarizations in CDP crystals.] (iii) The pressure effects on the Curie constant and the spontaneous polarization in CDP crystals are very striking in comparison with those in  $\text{KDP}$ ,<sup>10,11</sup>  $d$ - $\text{KDP}$ ,<sup>10,14</sup> and  $\text{RDP}$ .<sup>13</sup> (see Table I). (iv) The lack of an isotope effect on  $dT_c/dp$  for the paraelectric-ferroelectric transition in CDP is in marked contrast with the case of  $\text{KDP}$  where a large isotope effect on  $dT_c/dp$  exists (see Table I). On the other hand, the following facts have been clarified by neutron scattering studies on CDP and  $\text{KDP}$ .<sup>5,9</sup>: (a) the ordering of hydrogen atoms in the bonds associated with the zigzag chains running along the ferroelectric  $b$  axis plays an important role for the ferroelectric transition in CDP and exhibits one-dimensional characteristics, and the ferroelectric polarization is suggested to be due to the atomic displacements of heavy atoms along the chain triggered by this ordering of hydrogen atoms; and (b) the paraelectric-ferroelectric phase transition for  $\text{KDP}$  results from the strong three-dimensional ferroelectric correlation due to three-dimensional polarization fluctuations. Judging from the situation [(i)-(iii) and (a) and (b)] mentioned above, the paraelectric-ferroelectric phase transition for CDP results from weak three-dimensional ferroelectric correlation of polarizations among the chains along the  $b$  axis. Such a weak 3-D ferroelectric correlation ties to the 1-D nature of the phase transition in CDP.<sup>5,7</sup> Then the antiferroelectricity induced by a small pressure is inferred to originate in the 1-D characteristics with the chainlike ordering of the hydrogen bond along the  $b$  axis in CDP.<sup>5,7</sup> [see (a)]. Accordingly, the arrangement of polarizations along the  $b$  axis among

the nearest-neighbor chains is considered to be parallel in the ferroelectric phase and antiparallel in the antiferroelectric phase of CDP or *d*-CDP.

#### IV. DISCUSSION

The paraelectric-ferroelectric ( $T_c$ ) and the paraelectric-antiferroelectric transition temperature ( $T_n$ ) are increased largely by deuteration;  $T_c^d/T_c = 1.72$ , and  $T_n^d/T_n = 1.71$  at  $p_c^d$  or  $p_c$ , and these temperatures decrease with increasing pressure with slopes  $d \ln T_c/dp = -5.5\%/kbar$  and  $d \ln T_n/dp = -5.4\%/kbar$ , and such values for  $T_{c \text{ or } n}^d/T_{c \text{ or } n}$  and  $d \ln T_{c \text{ or } n}/dp$  are comparable with those for the other KDP-type ferroelectric and antiferroelectric crystals<sup>8,10</sup> (see Table I). These facts suggest that the proton on the hydrogen bond plays a central role for the phase transitions in the CDP crystal. Thus the CDP crystal belongs to the KDP-type hydrogen-bonded ferroelectric crystals. Here we adopt the tunneling model of the proton<sup>8,18-21</sup> accepted for KDP-type ferroelectrics as the microscopic mechanism for phase transitions in the CDP crystal, and we try to explain the dielectric properties of the CDP crystal by making use of the pseudospin formalism for KDP-type crystals.<sup>22,23</sup>

##### A. Paraelectric-ferroelectric phase transition

According to the modified tunneling model,<sup>21,23</sup> in the mean-field approximation the paraelectric-ferroelectric transition temperature ( $T_c$ ) is given by

$$2\Omega/J = \tanh(\Omega/2kT_c), \quad (1)$$

where  $\Omega$  is the proton tunneling integral,  $J$  is the proton-proton and lattice interaction constant, and  $k$  is the Boltzmann constant. The value of  $\Omega$  varies largely by deuteration, and the value of  $T_c$  is predicted to have a large isotope effect from Eq. (1). Moreover, the temperature dependence of the permittivity in the paraelectric phase is given by

$$\epsilon_0(\epsilon_r - 1) = \frac{4N\mu^2 \tanh(\Omega/2kT)}{[2\Omega - J \tanh(\Omega/2kT)]}, \quad (2)$$

where  $\epsilon_0$  is the vacuum permittivity and  $N$  is the number of dipole moments  $\mu$  per unit volume. The expansion of Eq. (2) around  $T_c$  yields the Curie constant  $C$  (Ref. 23)

$$C = 16N\mu^2 k T_c^2 / (J^2 - 4\Omega^2). \quad (3)$$

The spontaneous polarization  $P_s$  is given by

$$P_s = 2N\mu \langle S^z \rangle, \quad (4)$$

where  $\langle S^z \rangle$  is the expectation value of  $z$  component of a Pauli spin matrices of spin  $\frac{1}{2}$  and describes the ordering of the proton. In the paraelectric phase,

$\langle S^z \rangle = 0$  and then  $P_s = 0$ . Even at  $T \ll T_c$ , the spins do not align completely due to the finite tunneling probability of the proton, and thus the value of  $P_s$  is

$$P_s = N\mu(1 - 4\Omega^2/J^2)^{1/2}. \quad (5)$$

Let us examine the dielectric properties with the paraelectric-ferroelectric transition by the equations shown above. First, we determine the values of the important parameters  $J$  and  $\Omega$  in this model. By deuteration the transition temperature is largely increased and the value of tunneling integral ( $\Omega$ ) is decreased, so that  $\Omega^d/kT_c^d \ll 1$ . Thus,  $J^d = 4kT_c^d$  is obtained from Eq. (1). This relation and the measured value of  $T_c^d = 262$  K for *d*-CDP yield the value of  $J^d/k = 1048$  K. Furthermore, the relation of  $(J^d/J)^{1/2} = P_s^d/P_s$  is obtained by assuming that  $J$  is dominated by long-range forces and then represented as  $J \propto \mu^2$ ,<sup>24</sup> and then  $J/k = 728$  K is obtained by using the calculated value of  $J^d/k = 1048$  K and the value of  $P_s^d/P_s \cong 1.2$  extrapolated at  $T = 0$  K from the measured values of  $P_s^d$  and  $P_s$  up to 77 K in this work. So, substituting this value of  $J$  and  $T_c = 153$  K for CDP into Eq. (1), we can obtain  $\Omega/k = 235$  K, and this value is comparable with 253 K for KDP<sup>11</sup> and 233 K for RDP.<sup>25</sup> On the other hand, the decrease of  $T_c$  with pressure for KDP-type crystals is considered as follows<sup>8</sup>: As the pressure is applied to these materials, the O-H . . . O bond length becomes shorter and then both the height of the potential barrier and the separation between the two potential minima are expected to decrease. From an increase in the tunneling probability of the proton through the lower and narrower barrier, the decrease of  $T_c$  with pressure can result. Let us estimate the pressure dependence of the tunneling integral ( $\Omega$ ) from Eq. (1) by using the measured  $T_c(p)$  and  $T_c^d(p)$ . The pressure dependence of  $J^d$  is obtained from the measured  $T_c^d(p)$  dependence by using the relation of  $d \ln J^d/dp = d \ln T_c^d/dp$ . Although the value of  $J$  probably depends on deuteration, the logarithmic pressure derivative of  $J$  is assumed not to depend strongly on deuteration,<sup>13</sup> so  $d \ln J^d/dp \cong d \ln J/dp$ . The pressure dependence of  $\Omega$  can be obtained from Eq. (1) by using the value of  $\Omega$  at atmospheric pressure, the  $J(p)$  dependence obtained above and the measured  $T_c(p)$  dependence. The value of  $\Omega$  increases with pressure as seen in the inset in Fig. 1.

Since the mean-field approximation is known to fail in the ferroelectric phase at  $T < T_c$ ,<sup>19</sup> we deal with the permittivity in the paraelectric phase at  $T > T_c$ . The Eq. (2) indicates that the Curie-Weiss law holds goods at  $T$  around  $T_c$ , and the Curie constant ( $C$ ) is given by Eq. (3). The value of the dipole moment is calculated to be  $\mu = 2.3 \times 10^{-23}$   $\mu\text{C m}$  from Eq. (3) by using the measured value of  $C = 3.98 \times 10^{-7}$  K F/m at  $p = 1$  bar and the above values of model parameters, where the number of

dipole moments per unit volume is calculated to be  $N = 8.4 \times 10^{27}/\text{m}^3$  by using the specific gravity  $\rho = 3.2$ ,<sup>1</sup> because only one of the two kinds of O—H ··· O bond is associated with the transition in CDP and *d*-CDP.<sup>5,9</sup> As the volume compressibilities ( $\kappa$ ) for CDP and *d*-CDP have not been measured, we use the value of  $\kappa = -0.35\%/ \text{kbar}$  measured for other KDP-type crystals (KDP, *d*-KDP, and RDP).<sup>14,26</sup> The pressure dependence of the dipole moment ( $\mu$ ) is evaluated from both  $d \ln P_s / dp \cong -6\% / \text{kbar}$  measured for CDP and the relation of  $P_s = N\mu$ . By using the above values of model parameters, the Curie constant at  $p = 3$  kbar is calculated to be  $C = 3.09 \times 10^{-7}$  K F/m from Eq. (3). This calculated value is in good agreement with the measured value of  $C = 3.14 \times 10^{-7}$  K F/m. The  $\epsilon_r - T$  curves in the paraelectric phase under pressures calculated from Eq. (2) are shown as solid lines in Fig. 1. Moreover, the values of  $C^d$  for *d*-CDP at  $p = 1$  bar and  $p = 1$  kbar are calculated to be  $4.74 \times 10^{-7}$  K F/m and  $4.36 \times 10^{-7}$  K F/m, respectively, from Eq. (3) by using the relation of  $\Omega^d / kT_c^d \ll 1$ ,  $\mu^d / \mu \cong 1.2$  (measured) and  $d \ln \mu^d / dp$  obtained from  $d \ln P_s^d / dp \cong -4\% / \text{kbar}$  (measured) for *d*-CDP. These calculated values agree with the measured values of  $C^d = 5.22 \times 10^{-7}$  K F/m at  $p = 1$  bar and  $C^d = 4.87 \times 10^{-7}$  K F/m at  $p = 1$  kbar.

### B. Paraelectric-antiferroelectric phase transition

As clarified in the discussion on the experimental results in Sec. III B, the arrangement of polarizations in the pressure-induced antiferroelectric phase is made to be parallel within the hydrogen-bonded chain along the *b* axis and to be antiparallel among the nearest-neighbor chains, and the two sublattices of chains 1 and chains 2 are formed. In this case, the spin-spin interaction term ( $H_{ij}$ ) in the Hamiltonian given by the following expression should be applied<sup>22</sup>:

$$H_{ij} = -\left(\frac{1}{2}\right) \sum_{ij} [K_{ij}(S_{i1}^z S_{j1}^z + S_{i2}^z S_{j2}^z) + L_{ij} S_{i1}^z S_{j2}^z] \quad (6)$$

The indices 1 and 2 refer to the two sublattices,  $K_{ij}$  describes the spin-spin effective interaction constant within a given chain and  $L_{ij}$  is the effective interaction constant between spins on neighboring chains. According to Blinc *et al.*,<sup>22,23</sup> taking into account the tunneling term ( $\Omega$ ) and the external electric field term ( $E$ ), the thermal expectation values of the two sublattice polarizations ( $\langle S_1^z \rangle$  and  $\langle S_2^z \rangle$ ) are obtained in the mean-field approximation by solving the two coupled equations

$$\langle S_1^z \rangle = (H_{z1} / 2H_1) \tanh(H_1 / 2kT) \quad (7)$$

$$\langle S_2^z \rangle = (H_{z2} / 2H_2) \tanh(H_2 / 2kT) \quad (8)$$

where

$$H_1 = \{\Omega^2 + [K \langle S_1^z \rangle + (L/2) \langle S_2^z \rangle + 2\mu E]^2\}^{1/2} \quad ,$$

$$H_{z1} = K \langle S_1^z \rangle + (L/2) \langle S_2^z \rangle + 2\mu E \quad ,$$

$$H_2 = \{\Omega^2 + [K \langle S_2^z \rangle + (L/2) \langle S_1^z \rangle + 2\mu E]^2\}^{1/2}$$

and

$$H_{z2} = K \langle S_2^z \rangle + (L/2) \langle S_1^z \rangle + 2\mu E \quad .$$

In the antiferroelectric phase,  $\langle S_1^z \rangle = -\langle S_2^z \rangle$ , so the paraelectric-antiferroelectric transition temperature ( $T_n$ ) is obtained from the relation

$$2\Omega / (K - L/2) = \tanh(\Omega / 2kT_n) \quad . \quad (9)$$

The spontaneous polarization ( $P$ ) is obtained from the relation

$$P = N\mu(\langle S_1^z \rangle + \langle S_2^z \rangle) \quad . \quad (10)$$

In the paraelectric phase above  $T_n$ ,  $\langle S_1^z \rangle = \langle S_2^z \rangle = 0$ , and then the permittivity  $\epsilon = \epsilon_0 \epsilon_r$  is given from the relation of  $\epsilon_0(\epsilon_r - 1) = dP / dE_{E=0}$  as follows:

$$\epsilon_0(\epsilon_r - 1) = \frac{4N\mu^2 \tanh(\Omega / 2kT)}{[2\Omega - (K + \frac{1}{2}L) \tanh(\Omega / 2kT)]} \quad . \quad (11)$$

Expansion of Eq. (11) around  $T_n$  yields a Curie-Weiss law of the form

$$\epsilon(T) = C / (T - T_{n0}) \quad ,$$

with the Curie constant  $C$  given by

$$C = 16N\mu^2 k T_n^2 / [(K - L/2)^2 - 4\Omega^2] \quad . \quad (12)$$

The value of  $\epsilon_r$  at  $T_n$  is obtained by putting  $T_n$  in Eq. (9) into Eq. (11) as follows:

$$\epsilon_0(\epsilon_r - 1)_{T=T_n} = 4N\mu^2 / (-L) \quad . \quad (13)$$

Here the sign of  $L$  is negative because of the antiferroelectric interaction of spins between chain 1 and chain 2. The characteristic temperature ( $T_{n0}$ ) at which  $1/\epsilon_r = 0$  is obtained from Eq. (11) as follows:

$$2\Omega / (K + L/2) = \tanh(\Omega / 2kT_{n0}) \quad . \quad (14)$$

Let us examine the dielectric properties with the paraelectric-antiferroelectric transition for CDP and *d*-CDP by using the equations shown above. First we determine the values of the important model parameters of  $\Omega$ ,  $K$ , and  $L$ . The qualitative change from the paraelectric-ferroelectric to the paraelectric-antiferroelectric transition occurs at  $p_c = 3.3$  kbar for CDP. As known from considerations of vanishing of the ferroelectric and antiferroelectric states in KDP-type crystals at high pressure, especially from the discussion on the phase transition temperature,<sup>12</sup> there is no large discontinuous change in the tunneling integral at the phase boundary between ferroelectric and antiferroelectric phases. Therefore the value of  $\Omega/k = 249$  K at  $p_c$  estimated in the ferroelectric



TABLE II. The difference ( $\Delta T_n$  or  $\Delta T_n^d$ ) between the transition temperature and the characteristic temperature, the ferroelectric interaction constant ( $K$ ), and the antiferroelectric interaction constant ( $L$ ) of  $\text{CsH}_2\text{PO}_4$  and  $\text{CsD}_2\text{PO}_4$  under various pressures.

$p$ (kbar)	$\text{CsH}_2\text{PO}_4$			$\text{CsD}_2\text{PO}_4$		
	3.3 ( $p_c$ )	4.0	4.5	5.2 ( $p_c^d$ )	5.7	6.3
$\Delta T_n$ or $\Delta T_n^d$ (K) <sup>a</sup>	2.1	6.3	10.9	6.5	8.8	10.9
$K/k$ (K)	651.5	639.2	630.8	856.5	846.8	837.2
$L/k$ (K)	4.8	17.3	28.2	26.0	35.3	43.7

$$^a \Delta T_n = |T_n - T_{n0}| \text{ for } \text{CsH}_2\text{PO}_4, \Delta T_n^d = |T_n^d - T_{n0}^d| \text{ for } \text{CsD}_2\text{PO}_4.$$

phase should be also applicable for that at  $p_c$  in the antiferroelectric phase. By using this value of  $\Omega$  and the measured values of  $T_n$  and  $T_{n0}$  at  $p_c$ , the values of the parameters ( $K$  and  $L$ ) are estimated as shown in Table II from Eqs. (9) and (14). The Curie constant is estimated to be  $C = 3.08 \times 10^{-7}$  K F/m at  $p_c$  by using these values from Eq. (12), and this value of  $C$  is in agreement with the measured value of  $C = 3.26 \times 10^{-7}$  K F/m. Next let us estimate the pressure dependence of  $\Omega$  in the antiferroelectric phase. The pressure dependence of  $J_n^d \equiv (K - \frac{1}{2}L)^d$  is estimated from Eq. (9) by using the measured  $T_n^d(p)$  dependence and the relation of  $\Omega^d/kT_n^d \ll 1$ .<sup>13,24</sup> Although the value of  $J_n \equiv (K - \frac{1}{2}L)$  probably depends on deuteration, the logarithmic pressure derivative of  $J_n$  is assumed not to depend strongly on deuteration<sup>13</sup>; namely,

$$d \ln J_n / dp \cong d \ln J_n^d / dp \cong -1.2\% / \text{kbar}.$$

The above  $J_n(p)$  dependence and the measured  $T_n(p)$  dependence yield the  $\Omega(p)$  dependence from Eq. (9), and the calculated value of  $\Omega$  increases with pressure as seen at  $p > p_c$  in the inset in Fig. 1. Moreover, the values of the parameters of  $K$  and  $L$  estimated from Eqs. (9) and (14) by using the measured values of  $T_n$  and  $T_{n0}$  at  $p = 4.0$  and  $4.5$  kbar are shown in Table II. The  $\epsilon_r - T$  characteristics in the antiferroelectric phase are calculated from Eq. (11) by using the above values of model parameters, and are shown as solid lines in Fig. 1. The value of the Curie constant at  $p = 4.0$  kbar is estimated from Eq. (12) to be  $C = 3.16 \times 10^{-7}$  K F/m, where the value of  $d \ln \mu / dp$  estimated from the measured value of  $d \ln P_{\text{LH}}^d / dp \cong -1\% / \text{kbar}$  in the antiferroelectric phase was used. Although this value is a little less than the measured value of  $C = 4.16 \times 10^{-7}$  K F/m, the calculated positive pressure coefficient of  $C$  is qualitatively in agreement with the measured one. The condition of  $\Omega^d/kT_n^d \ll 1$  is applicable to the above Eqs. (9)–(14) for  $d$ -CDP, and the values of  $K$  and  $L$  estimated from Eqs. (9) and (14) by using the meas-

ured values of  $T_n^d$  and  $T_{n0}^d$  at various pressures are also shown in Table II. The  $\epsilon_r - T$  characteristics are calculated from Eq. (11) and are shown as solid lines in Fig. 2. Although the values of the Curie constant ( $C^d = 3.06 \times 10^{-7}$  K F/m at  $p = 5.2$  kbar and  $C^d = 2.99 \times 10^{-7}$  K F/m at  $p = 6.3$  kbar) estimated from Eq. (12) are a little less than the measured values ( $C^d = 4.24 \times 10^{-7}$  K F/m at  $p = 5.2$  kbar and  $C^d = 3.81 \times 10^{-7}$  K F/m at  $p = 6.3$  kbar), the calculated negative pressure coefficient of  $C^d$  is qualitatively in agreement with the measured one. Here, for the purpose of calculating  $\epsilon_r$  and  $C^d$ , the value of  $d \ln \mu^d / dp$  estimated from the measured value of  $d \ln P_{\text{LH}}^d / dp \cong -1\% / \text{kbar}$  was used.

As shown in Table II, the ferroelectric interaction constant  $K$  between spins within the chain along the  $b$  axis decreases with increasing pressure and the antiferroelectric interaction constant  $L$  between spins on neighboring chains increases rapidly with increasing pressure. This corresponds to the experimental results in this work that the value of  $P_{\text{LH}}$  corresponding to twice the magnitude of the spontaneous polarization of a sublattice<sup>16</sup> decreases and the critical electric field ( $E_{\text{cri}}$ ) increases rapidly, with increasing pressure. Therefore, with increasing pressure (i.e., decreasing distance between chains), one-dimensional ferroelectric correlation of polarizations within the chain along the  $b$  axis becomes weaker and the dipolar interaction among chains becomes stronger gradually, and its dipolar interaction seems to become dominant at pressures above the critical pressure ( $p_c$ ). So, the antiparallel dipolar arrangement seems to appear under the following consideration: Because the 3-D correlation of polarizations among the chains is weak (see Sec. IIIB), the polarizations along the chain may be simply treated as isolated dipoles,<sup>7</sup> and thus the dipolar interaction energy for the antiparallel arrangement of the two isolated dipole chains becomes lower than that for the parallel arrangement.<sup>27</sup> After that, the 3-D antiferroelectric correlation of polarizations among chains becomes stronger with increasing pressure.

Finally let us try to comment about the evaluation of the pressure dependence of the crucial parameters  $\Omega$  and  $J$  for paraelectric-ferroelectric and -antiferroelectric transitions. As was previously pointed out by Percy and Samara,<sup>13</sup> none of the parameters  $\Omega$  and  $J$  can be uniquely determined. The logarithmic pressure derivative for  $J$  was assumed to be similar to that of the  $T_c^d$  for the deuterated crystal. Then appreciable deviation of  $d \ln J / dp$  from the used value will not affect the qualitative evaluations, but will change the value of the initial slope of  $d \ln \Omega / dp$ . The values of  $d \ln \Omega / dp$  are estimated to be 2.7%/kbar for the paraelectric-ferroelectric transition and 4.0%/kbar for the paraelectric-antiferroelectric one (see Fig. 1). These values are larger than the value of  $d \ln \Omega / dp = 0.5\%/kbar$  for KDP,<sup>11,24,25</sup> but are the same order in the magnitude as the value of  $d \ln \Omega / dp \cong 4.9\%/kbar$  estimated for RDP.<sup>13</sup> In order to evaluate the pressure dependence of  $\Omega$  and  $J$  more precisely, a Raman scattering measurement under pressure must be performed. The lack of the isotope effect on  $dT_c/dp$  should be microscopically explained by the protonic order-disorder model, using a four-particle cluster approximation<sup>28</sup> instead of the present model using the mean-field approximation. Further experimental works such as the neutron scattering and x-ray diffraction studies under pressure must be made and further theoretical works dealing with the low-dimensional problems must be developed to clarify more the phase transition mechanism for CDP.

## V. CONCLUSIONS

The primary results and conclusions of this work on CDP and  $d$ -CDP are summarized as follows:

(i) For both compounds, the pressure-induced new phase is confirmed to be antiferroelectric by the observation of  $P$ - $E$  double hysteresis loops.

(ii) The pressure effect on the dielectric properties in both the ferroelectric and the antiferroelectric phases for CDP and  $d$ -CDP is found to be very large in comparison with that in the other KDP-type hydrogen-bonded crystals; the pressure dependence of (a) the spontaneous polarization and the Curie constant in the ferroelectric phase, and (b) the Curie constant, the value of  $\epsilon_r$  at  $T_n^{(d)}$ , and the critical electric field in the antiferroelectric phase are large for both compounds. Such facts are believed to be due to the weak 3-D correlation of polarizations, and reflect the 1-D nature characteristic of the chainlike ordering of hydrogen bonds along the  $b$  axis.

(iii) The dielectric properties associated with the paraelectric-ferroelectric and the paraelectric-antiferroelectric transitions are explained by introducing into an Ising spin model (containing the proton tunneling) a spin-spin interaction term within the chain and an interaction term between spins among the chains along the  $b$  axis.

(iv) The qualitative change from the paraelectric-ferroelectric to the paraelectric-antiferroelectric transition by a small pressure is interpreted to originate in the 1-D nature of CDP and  $d$ -CDP.

<sup>1</sup>Y. Uesu and J. Kobayashi, *Phys. Status Solidi A* **34**, 475 (1976).

<sup>2</sup>F. Seidl, *Tschermaks Mineral. Petrogr. Mitt.* **1**, 432 (1950).

<sup>3</sup>A. Levstik, R. Blinc, P. Kadaba, S. Cizikow, I. Levstik, and C. Pilipic, *Solid State Commun.* **16**, 1339 (1975).

<sup>4</sup>E. Kanda and T. Fujimura, *J. Phys. Soc. Jpn.* **43**, 1813 (1977).

<sup>5</sup>D. Semmingsen, W. D. Ellenson, B. C. Frazer, and G. Shirane, *Phys. Rev. Lett.* **38**, 1299 (1977).

<sup>6</sup>K. Gesi and K. Ozawa, *Jpn. J. Appl. Phys.* **17**, 435 (1978).

<sup>7</sup>N. Yasuda, M. Okamoto, H. Shimizu, S. Fujimoto, K. Yoshino, and Y. Inuishi, *Phys. Rev. Lett.* **41**, 1311 (1978).

<sup>8</sup>G. A. Samara, in *Advances in High Pressure Research*, edited by R. S. Bradely (Academic, New York, 1969), Vol. 3.

<sup>9</sup>R. J. Nelmes and R. N. P. Choudhary, *Solid State Commun.* **26**, 823 (1978).

<sup>10</sup>G. A. Samara, *Ferroelectrics* **20**, 87 (1978).

<sup>11</sup>P. S. Percy, *Phys. Rev.* **12**, 2725 (1975).

<sup>12</sup>G. A. Samara, *Phys. Rev. Lett.* **27**, 103 (1971).

<sup>13</sup>P. S. Percy and G. A. Samara, *Phys. Rev.* **8**, 2033 (1973).

<sup>14</sup>G. A. Samara, *Phys. Lett. A* **25**, 664 (1967).

<sup>15</sup>In KDP-type antipolar ADP, the ferroelectric phase has not been recognized to be induced by the application of electric field [see M. Marutake, in *Landolt-Bornstein:*

*Ferro- and Antiferroelectric Substances*, edited by T. Mitsui (Springer, Berlin, 1969), Vol. 3, p. 143]. Layered antiferroelectric cupric formate tetrahydrate characterized with the two-dimensional hydrogen-bonded network has a large critical electric field of about 10 kV/cm at 3°C below the transition temperature [see Ref. 16].

<sup>16</sup>K. Okada and H. Sugie, *J. Phys. Soc. Jpn.* **25**, 1128 (1968).

<sup>17</sup>V. H. Schmidt, A. B. Western, and A. G. Baker, *Phys. Rev. Lett.* **37**, 839 (1976).

<sup>18</sup>R. Blinc, *J. Phys. Chem. Solids* **13**, 204 (1960); P. G. de Gennes, *Solid State Commun.* **1**, 132 (1963).

<sup>19</sup>R. Blinc and S. Svetina, *Phys. Rev.* **147**, 430 (1966).

<sup>20</sup>M. Tokunaga and T. Matsubara, *Prog. Theor. Phys.* **35**, 581 (1966); **36**, 857 (1966).

<sup>21</sup>K. K. Kobayashi, *J. Phys. Soc. Jpn.* **24**, 497 (1968).

<sup>22</sup>R. Blinc, H. Arend, and A. Kanduser, *Phys. Status Solidi B* **74**, 425 (1976).

<sup>23</sup>R. Blinc and B. Žekš, *Adv. Phys.* **29**, 693 (1972).

<sup>24</sup>P. S. Percy, *Phys. Rev. B* **13**, 3945 (1976).

<sup>25</sup>P. S. Percy, *Phys. Rev.* **9**, 4868 (1974).

<sup>26</sup>B. Morosin and G. A. Samara, *Ferroelectrics* **3**, 49 (1971).

<sup>27</sup>See, for example, F. Jona, and G. Shirane, *Ferroelectric Crystals* (Pergamon, Oxford, 1962), p. 24.

<sup>28</sup>R. Blinc and B. Žekš, *Phys. Lett. A* **26**, 468 (1968); *Helv. Phys. Acta.* **41**, 700 (1968).

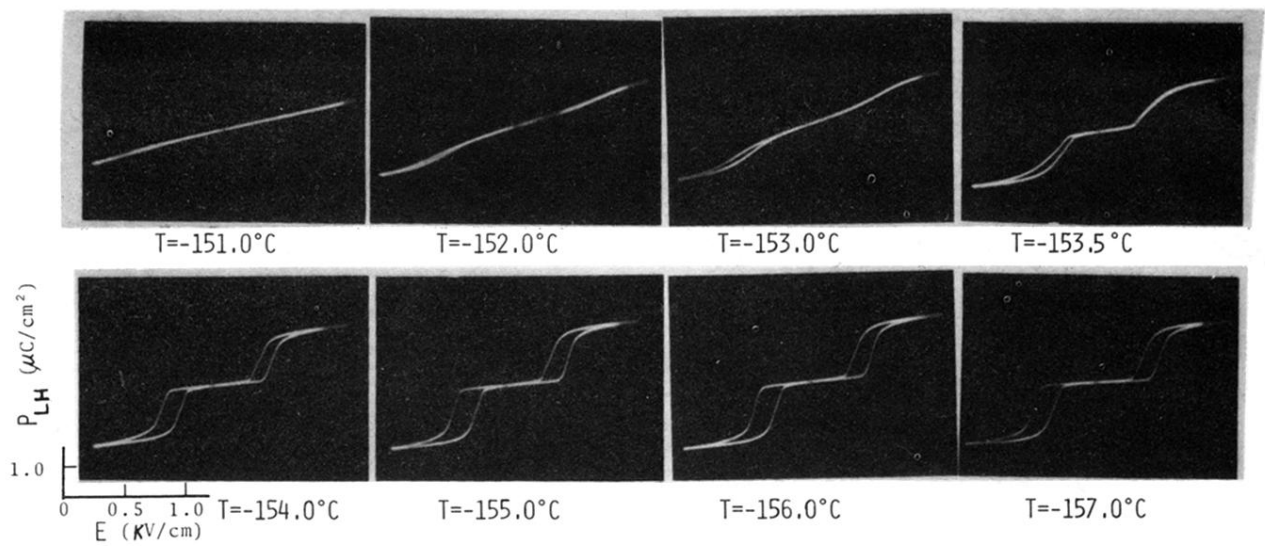


FIG. 5.  $P$ - $E$  double hysteresis loops at  $p = 3.7$  kbar with an ac amplitude of  $1.1$  kV/cm, along the  $b$  axis of  $\text{CsH}_2\text{PO}_4$  at various temperatures.

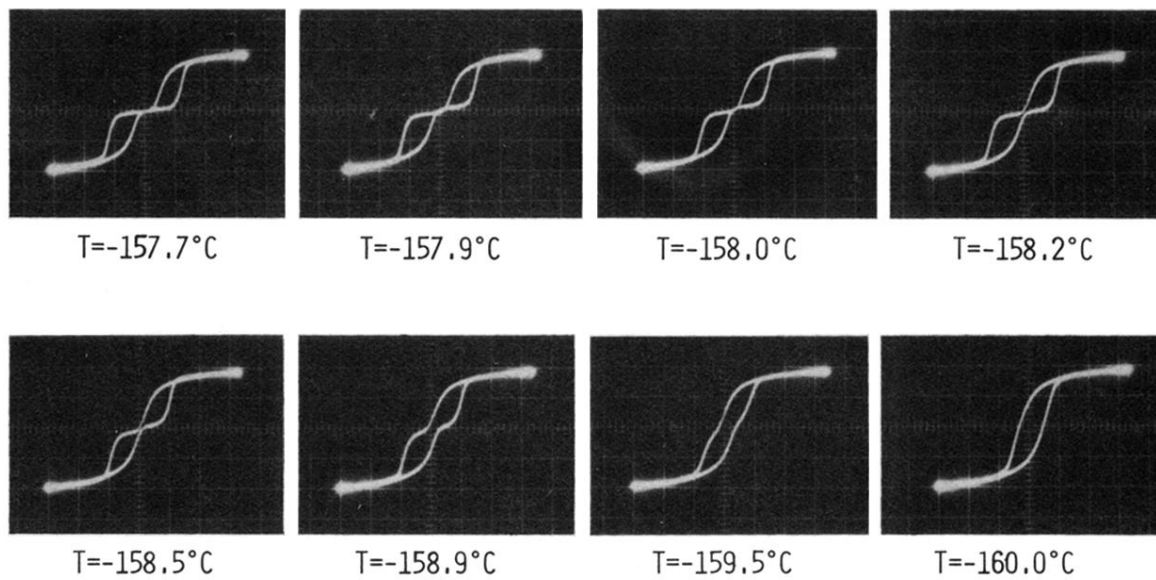


FIG. 8.  $P$ - $E$  relation of the antiferroelectric phase to the ferroelectric one along the  $b$  axis of  $\text{CsH}_2\text{PO}_4$  at the pressure just above  $p_c$  with cooling.